The nature of monomer inversion in the ammonia dimer

E. H. T. Olthof, A. van der Avoird, and P. E. S. Wormer
Institute of Theoretical Chemistry, University of Nijmegen, Toernooiveld, 6525 ED Nijmegen, The Netherlands

J. G. Loeser and R. J. Saykally
Department of Chemistry, University of California, Berkeley, California 94720

(Received 13 June 1994; accepted 9 August 1994)

A model is presented for calculating the splittings due to umbrella inversion of the monomers in $(NH_3)_2$. Input to the model are the six-dimensional dimer bound state wave functions for rigid monomers, calculated previously [E. H. T. Olthof, A. van der Avoird, and P. E. S. Wormer, J. Chem. Phys. **101**, 8430 (1994)]. This model is based on first-order (quasi) degenerate perturbation theory and adaptation of the wave functions to the group chain $G_{36} \subset G_{72} \subset G_{144}$. The umbrella inversion splittings depend sensitively on the intermolecular potential from which the bound state wave functions are obtained. A complete interpretation of the observed splitting pattern [J. G. Loeser, C. A. Schmuttenmaer, R. C. Cohen, M. J. Elrod, D. W. Steyert, R. J. Saykally, R. E. Bumgarner, and G. A. Blake, J. Chem. Phys. **97**, 4727 (1992)] and quantitative agreement with the measured splittings, which range over three orders of magnitude, are obtained from the potential that reproduces the far-infrared spectrum of $(NH_3)_2$ and the dipole moment and nuclear quadrupole splittings of $(NH_3)_2$ and $(ND_3)_2$. The umbrella inversion splittings of $(ND_3)_2$ are predicted.

I. INTRODUCTION

The umbrella inversion of the free NH_3 molecule is a well-studied[1] phenomenon. Quantum mechanically, the inversion is described by a tunneling through the barrier of the NH_3 double well potential. This tunneling gives rise to an energy splitting of states that, without the tunneling, would be degenerate and would be localized on either side of the potential barrier. Through the interaction with another monomer the tunneling may or may not be quenched. For example, in the case of the NH_3–Ar van der Waals molecule the tunneling splitting is hardly affected in most of the rovibrational states, but in some states it is nearly quenched.[2,3]

The spectrum of the $(NH_3)_2$ dimer was first observed by Nelson, Fraser, and Klemperer[4] in the microwave region. These workers interpreted their spectrum by assuming that the monomers constituting the dimer are rigid and noninverting. However, later far-infrared measurements by Loeser *et al.*[5] and infrared–far-infrared double resonance experiments by Havenith *et al.*[6] showed energy splittings that were ascribed to incompletely quenched umbrella inversions of the monomers. These measurements demonstrate that, although monomer inversion in the dimer is about 10 times slower than in free ammonia, it is still observable.

In this paper we will address the question whether computations can account for the observed splittings and, in particular, whether the interpretation of the measurements in Refs. 5 and 6 can be supported theoretically. Furthermore, we will see that the splittings depend very sensitively on the intermolecular potential, so that they offer an accurate check on its validity. In the accompanying paper,[7] we report vibration–rotation-tunneling (VRT) calculations on the ammonia dimer, in which we freeze all internal monomer coordinates. This requires the solution of a Schrödinger equation depending on six degrees of freedom: the intermolecular distance R and the five internal Euler angles of the dimer. Ideally, we would now introduce the monomer umbrella angles as two extra degrees of freedom and solve the ensuing eight-dimensional Schrödinger equation. However, such a calculation is beyond present-day computer capabilities, which is why we resort to the simplified model that we used and tested earlier[3] on NH_3–Ar. Briefly, the model can be described as degenerate first order perturbation theory. The degenerate set of zeroth-order states consists of a van der Waals state, obtained from the solution of the six-dimensional (in NH_3–Ar a three-dimensional) Schrödinger equation, multiplied by the lowest two inversion ("umbrella") states of each free ammonia. The perturbation is the part of the Hamiltonian that describes the tunneling through the ammonia double well potentials. The van der Waals states are separated typically by about 20 cm^{-1}, whereas the unquenched umbrella splitting is 0.8 cm^{-1}. One can expect, therefore, that a first-order approximation is reasonable. Indeed, by comparison with results of four-dimensional VRT calculations on NH_3–Ar we found the model to be quite accurate.[8] In this work we extend the model to the $(NH_3)_2$ dimer by multiplying each van der Waals state by four umbrella functions, two on each center. Furthermore, we will see that in a few cases the van der Waals states are very close in energy. In those cases we apply quasidegenerate first-order perturbation energy.

Instead of numerically diagonalizing the first-order perturbation matrices, we will apply group theory to diagonalize the matrices. We not only do this because it is a compact and elegant approach, but mainly because Loeser *et al.* provide group theoretical labels for their observed levels and we wish to connect the present theoretical work with the earlier experimental work.

II. SYMMETRY ADAPTATION

We label the protons on monomer A by 1,2,3, and the protons on monomer B by 4,5,6. The nitrogen atoms of the

TABLE I. The groups C_{3v}^{ag} and C_{3v}^{g}. Note that $C_{3v}^{ag} = C_3^{ag}\circledS\{E,I_{ag}\}$ and $C_{3v}^{g} = C_3^{g}\circledS\{E,I_g^*\}$.

C_{3v}^{ag}		C_{3v}^{g}	
C_3^{ag}	(1)	C_3^{g}	(1)
	(123)(465)		(123)(456)
	(132)(456)		(132)(465)
K^{ag}	$I_{ag}\equiv$(14)(25)(36)(78)	K^{g}	$I_g^*\equiv$(14)(26)(35)(78)*
	(16)(24)(35)(78)		(15)(24)(36)(78)*
	(15)(26)(34)(78)		(16)(25)(34)(78)*

monomers A and B have labels 7 and 8, respectively. The group of feasible permutations inversions (PI's) of two noninverting monomers is generated by (123)(456), equivalent to a "geared" rotation of both monomers A and B over 120° around their C_3 axes, (132)(456) an 'antigeared' rotation of monomers A and B, the permutation I_{ag}=(14)(25)(36)(78) interchanging monomer A and B, and the interchange operator $I_g^* = (14)(26)(35)(78)^*$ that is a product of a permutation and space inversion E^*. This group of order 36 is designated[9] by G_{36} and can be written as the outer direct product $C_{3v}^{ag} \otimes C_{3v}^{g}$ (see Table I). The generators I_{ag} and I_g^* are labeled in correspondence with the subgroups to which they belong. When umbrella inversion is considered to be feasible, two more permutations must be added to the list of generators. We could, e.g., choose (23), which inverts A and (56), which inverts B, but other choices of coset generators are possible. The total PI group is then G_{144}, which is of order 144. In this section we will discuss how we can adapt products of van der Waals states and umbrella functions to the group G_{144}, while knowing that the van der Waals states span irreducible representations (irreps) of its subgroup G_{36}. We will achieve this by the group theoretical process of induction along a canonical chain[10] of subgroups of G_{144}. Recall that in a canonical chain all inductions and subductions are multiplicity free and that the chain starts with an Abelian subgroup. This implies that the basis functions of G_{144} can uniquely (up to phase and normalization) be defined by "sequence adapting"[10] the functions to the chain, or in other words, by specifying according to which irreps of the subgroups in the chain the functions transform.

First we introduce $G_{72}=G_{36}\otimes\{E,E^*\}$ and then note that G_{144} is a semidirect product,

$$G_{144}=G_{72}\circledS\{E,(56)\}.$$

The group G_{36} equals $C_{3v}^{ag} \otimes C_{3v}^{g}$, and the "antigeared" and "geared" groups are given in Table I. Both groups are isomorphic to C_{3v} and are themselves also semidirect products. Introducing $P_{18} \equiv C_{3v}^{ag} \otimes C_3^{g}$, we find the canonical chain

$$G_{144}\supset G_{72}\supset G_{36}\supset P_{18}\supset C_3^{ag}\otimes C_3^{g},$$

which will aid us in the adaptation of the basis.

The Hamiltonian H_{vdw}, which does not contain any terms depending on internal monomer coordinates, is taken as the zeroth-order Hamiltonian in the present work; see Refs. 7 and 11 for its explicit definition. The van der Waals states, adapted to G_{36}, are obtained by diagonalizing this Hamiltonian in the following basis of coupled rotor functions,

$$|j_A,k_A,j_B,k_B,j,K,J,M\rangle,$$

where the indices are running as

$$j_A,j_B=0,\ldots,j_{\max},\quad j=|j_A-j_B|,\ldots,j_A+j_B,$$

$$|K|=0,\ldots,\min(j,J),$$

$$k_A=-j_A,\ldots,j_A,\quad k_B=-j_B,\ldots,j_B.$$

The quantum numbers J and M are strictly conserved and K is an approximate constant of the motion only broken by the weak Coriolis coupling. Although we have included the Coriolis coupling in the final stage of our calculations in Ref. 7, it gives only little mixing of the functions with different K and one can still use K to label the van der Waals states. See Refs. 7 and 11 for the explicit definition of the basis. In this work we are only concerned with its transformation properties under G_{144}. In Ref. 12 it is described how these transformations may be determined and they are listed in Table II. The eigenfunctions of H_{vdw} of energy $\mathscr{E}_i^{\gamma}$ have the form

$$\psi_{a,i}^{\gamma}=\sum_{\{\Lambda\},n}{}'C_{\{\Lambda\},n;i}^{\gamma}P_a^{\gamma}|\{\Lambda\},J,M,n\rangle,$$

$$\text{with}\quad a=1,\ldots,f_{\gamma},$$

where γ indicates an f_γ dimensional irrep of G_{36}, $\{\Lambda\}=\{j_A,k_A,j_B,k_B,j,K\}$, and n runs over the radial functions. The projectors P_a^{γ} are given in Ref. 11, and will be rederived below. The prime on the summation indicates that the indices are restricted, so that the sum is over a linearly independent set. By introducing a new set of coefficients

$$c_{\{\Lambda\},n;i}^{\gamma}=\sum_{\{\Lambda'\}}{}'C_{\{\Lambda'\},n;i}^{\gamma}\langle\{\Lambda\},J,M,n|P_a^{\gamma}|\{\Lambda'\},J,M,n\rangle,$$

TABLE II. Transformation properties of the basis functions under several permutation inversions.

PI	Effect on basis	
(123)	$\exp(2\pi ik_A/3)$	$\|j_Ak_Aj_Bk_Bj KJMn\sigma_A\sigma_B\rangle$
(456)	$\exp(2\pi ik_B/3)$	$\|j_Ak_Aj_Bk_Bj KJMn\sigma_A\sigma_B\rangle$
I_{ag}=(14)(25)(36)(78)	$(-1)^{J+j_A+j_B}$	$\|j_Bk_Bj_Ak_Aj -KJMn\sigma_B\sigma_A\rangle$
I_g^*=(14)(26)(35)(78)*	$(-1)^{j+k_A+k_B}$	$\|j_B-k_Bj_A-k_Aj KJMn\sigma_B\sigma_A\rangle$
(23)	$(-1)^{j_A}$	$\|j_A-k_Aj_Bk_Bj KJMn-\sigma_A\sigma_B\rangle$
(56)	$(-1)^{j_B}$	$\|j_Ak_Aj_B-k_Bj KJMn\sigma_A-\sigma_B\rangle$
E^*	$(-1)^{J+j+k_A+k_B}$	$\|j_Ak_Aj_Bk_Bj -KJMn-\sigma_A-\sigma_B\rangle$

we can write the VRT state as an unrestricted summation over primitive basis functions

$$\psi^{\gamma}_{a,i}=\sum_{\{\Lambda\},n} c^{\gamma}_{\{\Lambda\},n;i}|\{\Lambda\},J,M,n\rangle.$$

Because the matrix element of P^{γ}_{a} contains many Kronecker deltas the new coefficients $c^{\gamma}_{\{\Lambda\},n;i}$ are simple linear combinations of the coefficients $C^{\gamma}_{\{\Lambda\},n;i}$. As long as we neglect Coriolis coupling, the sum over $\{\Lambda\}$ is restricted to a single value of K. The ammonia monomer inversion is treated as a perturbation. This motion, depending on the angle ρ_X between the N–H bonds of monomer X and its three-fold symmetry axis, is described by Papoušek *et al.*[1] who give a Hamiltonian $H_{\rm inv}(\rho_X)$. In terms of their Hamiltonian the perturbation is

$$V=H_{\rm inv}(\rho_A)+H_{\rm inv}(\rho_B). \tag{1}$$

The lowest two eigenfunctions of $H_{\rm inv}(\rho)$, written as $\psi^{\pm}(\rho)$, are separated by the small energy difference $\Delta=0.793$ $\rm cm^{-1}=23.8$ GHz.[13] The next levels are about 950 $\rm cm^{-1}$ higher, and so we consider only the lowest two on each monomer. Rather than using these functions directly, we take the following linear combinations

$$f_{\pm}(\rho)\equiv|\pm\rangle=[\psi^{+}(\rho)\pm\psi^{-}(\rho)]/\sqrt{2}. \tag{2}$$

The function $|+\rangle\equiv f_{+}$ describes a vibrational state of the monomer localized in the right-hand potential well with umbrella up, and $|-\rangle\equiv f_{-}$ is localized in the left-hand well, umbrella down; note that $f_{+}(\pi-\rho)=f_{-}(\rho)$. When we performed the six-dimensional (zeroth-order) calculations, each NH_3 molecule was locked in one of the two umbrella wells, which is why we must localize our zeroth-order umbrella functions. The total unperturbed wave functions can be written as $|\psi^{\gamma}_{a,i},\sigma_A,\sigma_B\rangle$, where $\sigma_A=\pm$ and $\sigma_B=\pm$ refer to a given (up or down) structure of the two umbrellas and $\psi^{\gamma}_{a,i}$ is the corresponding six-dimensional van der Waals wave function calculated for the fixed umbrellas. Since the umbrellas are inverted by the permutations (23) and (56), the degenerate set of unperturbed functions is

$$g|\psi^{\gamma}_{a,i},\sigma_A,\sigma_B\rangle,\quad \text{with } g\in\{E,(23),(56),(23)(56)\},$$
$$a=1,\ldots,f_{\gamma}.$$

Our first order perturbation model implies that $V=H_{\rm inv}(\rho_A)+H_{\rm inv}(\rho_B)$ is diagonalized in the space of these degenerate functions. Or, equivalently, that the total Hamiltonian $H=H_{\rm vdw}+V$ is diagonalized in the same space. We prefer the latter formulation because it is possible then to generalize the model to quasidegenerate van der Waals states by simply extending the space of unperturbed functions in which H is diagonalized. There is a formal problem, however, which is similar to the problem met in symmetry adapted perturbation theory.[14] The symmetry group G_{144} of the total (perturbed) Hamiltonian is larger than the symmetry group G_{36} of the unperturbed Hamiltonian $H_{\rm vdw}$. This is because in the total Hamiltonian the umbrella coordinates ρ_A and ρ_B are considered as variables, whereas in $H_{\rm vdw}$ they are clamped at their equilibrium values. In fact, the perturbation is not simply the operator $H_{\rm inv}(\rho_A)+H_{\rm inv}(\rho_B)$, but also the difference between $H_{\rm vdw}(\mathbf{x},\rho_{\rm A},\rho_{\rm B})$ for variable ρ_A, ρ_B and $H_{\rm vdw}(\mathbf{x},\rho^{\rm e}_{\rm A},\rho^{\rm e}_{\rm B})$ for the equilibrium configurations of the umbrellas. Here $\mathbf{x}$ stands for the other six internal coordinates. Our model assumes, however, that the functions $f_{\pm}(\rho)$ are well localized and that in the region of localization $H_{\rm vdw}(\mathbf{x},\rho^{\rm e}_{\rm A},\rho^{\rm e}_{\rm B})\approx H_{\rm vdw}(\mathbf{x},\rho_{\rm A},\rho_{\rm B})$. Hence, the matrix elements of these functions over the difference operator will be neglected.

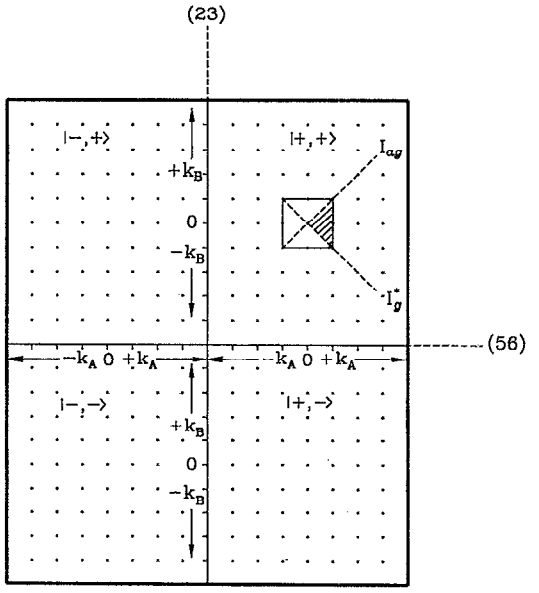

FIG. 1. The restriction of the symmetry adapted basis. Each "lattice" point depicts $|k_A,k_B\rangle\equiv|j_Ak_Aj_Bk_Bj KJM\rangle|\sigma_A,\sigma_B\rangle$, for certain fixed j_A, j_B, j, K, J, and M. The effect of the G_{144} generators is indicated: (23) gives a reflection in the y axis and (56) in the x axis, so that only the first quadrant with $|\sigma_A,\sigma_B\rangle=|+,+\rangle$ has to be considered. Restriction of k_A and k_B to values identical mod 3 gives the "unit cell" shown in the first quadrant. Within the unit cell the generators $I_{\rm ag}$ and I^*_g act as mirror planes, thus giving a further reduction of the range of k_A and k_B.

In principle j_A, k_A, j_B, k_B, j, and K run independently over their respective ranges. However, when we adapt the basis functions to G_{144} by projecting with linear combinations of the generators, we must ascertain that we do not generate linear dependencies and, conversely, we must be careful not to omit any functions. To this end we depict in Fig. 1 the basis as a lattice of points. Each point is labeled by a pair (k_A,k_B) with $-j_X\leq k_X\leq j_X$, $X=A,B$ and certain fixed j_A, j_B, j, and K (in Fig. 1, $j_A=3$ and $j_B=4$). The first quadrant contains all $|+,+\rangle$, the second all $|-,+\rangle$, the third all $|-,-\rangle$, and the fourth quadrant contains all $|+,-\rangle$ kets. As follows from the action of (23) on the basis functions given in Table II, a point in the first and fourth quadrant is reflected in the y axis by this G_{144} generator. Likewise, (56) maps points in the first/second quadrant onto the fourth/third quadrant. So when acting with (23) and (56) on all basis functions, we must restrict the basis to one quadrant, say the first, i.e., to kets $|+,+\rangle$.

All functions with the same value for (k_A,k_B) (mod 3) belong to the same irrep of the Abelian group $C^{ag}_3\otimes C^{g}_3$, since this group is isomorphic to $C^{A}_3\otimes C^{B}_3$, generated by (123) and (456), and k_A and k_B are symmetry labels of the latter direct

TABLE III. Basis functions adapted to $C_3^{ag} \otimes C_3^g$.

$\|0,0\rangle$	$A_1 \otimes A_1$
$\|-1,1\rangle$	$A_2 \otimes A_1$
$\|1,-1\rangle$	$A_3 \otimes A_1$
$\|1,0\rangle$	$A_2 \otimes A_2$
$\|-1,-1\rangle$	$A_1 \otimes A_2$
$\|1,1\rangle$	$A_1 \otimes A_3$
$\|0,-1\rangle$	$A_2 \otimes A_3$
$\|0,1\rangle$	$A_3 \otimes A_2$
$\|-1,0\rangle$	$A_3 \otimes A_3$

TABLE IV. Basis functions adapted to $G_{36} = C_{3v}^{ag} \otimes C_{3v}^g$. Partner functions are obtained by the generators given between square brackets acting on the same ket. The shorthand notation $|k_A,k_B\rangle \equiv |j_A k_A j_B k_B j K J M n\rangle |+,+\rangle$ is used, where the k values are unique modulo 3. The action of I_{ag} and I_g^* is given in Table II. The irreps of G_{36} are labeled according to Ref. 9.

$[E](E + I_{ag})(E + I_g^*)$	$\|0,0\rangle$	$A_1 = A_1 \otimes A_1$
$[E](E - I_{ag})(E + I_g^*)$	$\|0,0\rangle$	$A_2 = A_2 \otimes A_1$
$[E](E + I_{ag})(E - I_g^*)$	$\|0,0\rangle$	$A_3 = A_1 \otimes A_2$
$[E](E - I_{ag})(E - I_g^*)$	$\|0,0\rangle$	$A_4 = A_2 \otimes A_2$
$[E,I_{ag}](E + I_g^*)$	$\|1,-1\rangle$	$E_1 = E \otimes A_1$
$[E,I_{ag}](E - I_g^*)$	$\|1,-1\rangle$	$E_2 = E \otimes A_2$
$[E,I_g^*](E + I_{ag})$	$\|1,1\rangle$	$E_3 = A_1 \otimes E$
$[E,I_g^*](E - I_{ag})$	$\|1,1\rangle$	$E_4 = A_2 \otimes E$
$[E,I_{ag},I_g^*,I_{ag}I_g^*]$	$\|1,0\rangle$	$G = E \otimes E$

product group. Therefore, instead of looking at the entire sublattice of $(2j_A+1)\times(2j_B+1)$ functions, it suffices to consider only the "unit cell" spanned by $-1 \leq k_A \leq 1$ and $-1 \leq k_B \leq 1$. Suppressing J and M in the notation, we see that the generator I_{ag} maps $|j_A,k_A,j_B,k_B,j,K,+,+\rangle$ onto $|j_B,k_B,j_A,k_A,j,-K,+,+\rangle$, which, in general, is in a "unit cell" in the first quadrant of a lattice with different j_A, j_B, and K. Since j_A, j_B, j, and K are running independently, this lattice is also included in our basis and we do not distinguish between these two lattices in Fig. 1. We then see that I_{ag} reflects points within the unit cell in the $k_A = k_B$ line, so that the basis can be restricted to $k_B \leq k_A$. Similarly, since I_g^* maps $|j_A,k_A,j_B,k_B,j,K,+,+\rangle$ onto $|j_B,-k_B,j_A,-k_A,j,K,+,+\rangle$, we can apply the restriction $k_B \geq -k_A$. Combining the latter two restrictions, we find that $-k_A \leq k_B \leq k_A$. Note that this implies that $k_A \geq 0$ and that it is sufficient to consider kets with pairs $(k_A,k_B)=(0,0)$, $(1,0)$, $(1,1)$, and $(1,-1)$ in the symmetry adaptation of the basis. In the notation used in the remainder of this section we will suppress all other quantum numbers. The interchange operator I_{ag} also changes K into $-K$. Hence, if $k_A = k_B$ we may further impose the restriction $K \geq 0$. In the following, it will be shown that this holds for the A_1,A_2,A_3,A_4 irreps of G_{36} with $(k_A,k_B)=(0,0)$ and for the E_3,E_4 irreps with $(k_A,k_B)=(1,1)$.

For readers not familiar with the construction of irreps for semidirect product groups, we summarize in the Appendix this construction for the present simple case where the second factor is of order 2. For the general formalism we refer to Ref. 15. As a first example of the use of a semidirect product, we consider the construction of irreps of C_{3v}^{ag} and C_{3v}^g from those of C_3^{ag} and C_3^g. In Table III we find the basis functions adapted to $C_3^{ag} \otimes C_3^g$. From Table III we derive Table IV, the functions adapted to G_{36}. Let us first consider the induction $C_3^{ag} \otimes C_3^g \uparrow P_{18} \equiv C_{3v}^{ag} \otimes C_3^g$ by adding the coset generator I_{ag}. From the structure of the irreps of a cyclic group follows that A_3 of C_3^{ag} is obtained by inverting the elements in the irrep A_2. Furthermore, it follows from Table I that $I_{ag}\pi I_{ag} = \pi^{-1}$, with $\pi \in C_3^{ag}$. Therefore, π acting on $|1,-1\rangle$ gives the 1×1 matrices in the $A_3 \otimes A_1$ irrep and $I_{ag}\pi I_{ag}$ acting on the same function gives matrices from $A_2 \otimes A_1$. Therefore, the functions $|1,-1\rangle$ and $I_{ag}|1,-1\rangle$ span a two-dimensional irrep. If we next induce to G_{36} by adding I_g^*, we find that $\tau \in C_3^g$ and $I_g^* \tau I_g^*$ yield the same matrices (A_1). As we show in the Appendix, we must then act with $E \pm I_g^*$ and thus obtain the irreps of G_{36}, designated by E_1 and E_2 in Table IV. By inspection we find that the plus combination belongs to A_1 of C_{3v}^g and the minus combination to A_2. The functions transforming as $A_2 \otimes A_2$ and $A_3 \otimes A_2$ of $C_3^{ag} \otimes C_3^g$ give rise to $E \otimes A_2$ of P_{18}, i.e., $|1,0\rangle$ and $I_{ag}|1,0\rangle$ span this irrep. Likewise $I_g^*|1,0\rangle$ and $I_{ag}I_g^*|1,0\rangle$ span the irrep $E \otimes A_3$. Together these four functions span $E \otimes E = G$ of G_{36}. The rest of Table IV follows from equivalent arguments. We observe, since the A_1, A_2, A_3, A_4 and E_3, E_4 bases are projected by $E \pm I_{ag}$, that these basis functions are combinations of functions with K and functions with $-K$. Hence, the states that belong to these irreps may be labeled with $|K|$. For the E_1, E_2, and G irreps, the states with K should be distinguished from those with $-K$.

The step to G_{72} is simple: We project all kets in Table IV by $E \pm E^*$ and give the corresponding superscripts $\pm$ to the G_{36} irrep labels. From Table IV we derive Table V by adding the coset generator (56). In order to explain how to proceed, we label the elements in the rows of Table I by h_i^{ag} and h_i^g, $i=1,\ldots,6$. By their very construction, the irreps of these C_{3v} groups are identical: $\mathbb{D}(h_i^{ag})^\gamma = \mathbb{D}(h_i^g)^\gamma$. We have here the case discussed in general terms at the end of the Appendix, but with one modification, which is due to the fact that G_{72} is not invariant under (56). By inspection of Table I, we see that $(56)h_i^{ag}h_j^g(56) = h_j^{ag}h_i^g$, provided $h_i^{ag} \in C_3^{ag}$ and $h_i^g \in C_3^g$. However, when either $h_i^{ag} \in K^{ag}$ or $h_i^g \in K^g$, then $(56)h_i^{ag}h_j^g(56) = h_j^{ag}h_i^g E^*$, an element outside G_{36}. When $h_i^{ag} \in K^{ag}$ and simultaneously $h_i^g \in K^g$, then $(56)h_i^{ag}h_j^g(56) = h_j^{ag}h_i^g$. The same classification can be made for the coset of G_{36} in G_{72} generated by E^*. The appearance of the inversion E^*, in the products transformed by (56), is of no importance for the positive parity irreps of G_{72} designated by $(\gamma \otimes \gamma')^+$, where γ and γ' label the irreps of C_{3v}^{ag} and C_{3v}^g, respectively. The theory at the end of the Appendix applies without change and so

$$(56):(\gamma \otimes \gamma')^+ \mapsto (\gamma' \otimes \gamma)^+.$$

The negative parity irreps $(\gamma \otimes \gamma')^-$, however, are multiplied by -1 when either $h^{ag} \in K^{ag}$ or $h^g \in K^g$. Remembering that the A_2 representation of C_{3v}^{ag} has a character $+1$ for $h^{ag} \in C_3^{ag}$ and -1 for $h^{ag} \in K^{ag}$, and likewise for C_{3v}^g, we see that

$$(56):(\gamma \otimes \gamma')^- \mapsto [(A_2 \otimes \gamma') \otimes (A_2 \otimes \gamma)]^-.$$

We must project with $E \pm (56)$, when (56) maps onto an equivalent irrep (in the case that both γ and γ' are more-

TABLE V. The sequence adapted basis for G_{144}. The G_{144} irreps are, apart from parity, labeled according to Odutola *et al.* (Ref. 16). The partners of the irreps that occur twice span identical matrix representations. See Table IV for the definition of the shorthand notation used.

G_{144}	$\supset G_{36}$	Partners	Sequence adapted ket
A_1^+	A_1	$[E]$	$(E+E^*)[E+(56)](E+I_{ag})(E+I_g^*)\|0,0\rangle$
A_1^-	A_3	$[E]$	$(E-E^*)[E+(56)](E+I_{ag})(E-I_g^*)\|0,0\rangle$
A_2^+	A_4	$[E]$	$(E+E^*)[E-(56)](E-I_{ag})(E-I_g^*)\|0,0\rangle$
A_2^-	A_2	$[E]$	$(E-E^*)[E-(56)](E-I_{ag})(E+I_g^*)\|0,0\rangle$
B_1^+	A_4	$[E]$	$(E+E^*)[E+(56)](E-I_{ag})(E-I_g^*)\|0,0\rangle$
B_1^-	A_2	$[E]$	$(E-E^*)[E+(56)](E-I_{ag})(E+I_g^*)\|0,0\rangle$
B_2^+	A_1	$[E]$	$(E+E^*)[E-(56)](E+I_{ag})(E+I_g^*)\|0,0\rangle$
B_2^-	A_3	$[E]$	$(E-E^*)[E-(56)](E+I_{ag})(E-I_g^*)\|0,0\rangle$
E^+	$A_2\oplus A_3$	$[E,(56)]$	$(E+E^*)(E-I_{ag})(E+I_g^*)\|0,0\rangle$
E^+	$A_2\oplus A_3$	$[(56),E]$	$(E+E^*)(E+I_{ag})(E-I_g^*)\|0,0\rangle$
E^-	$A_1\oplus A_4$	$[E,(56)]$	$(E-E^*)(E+I_{ag})(E+I_g^*)\|0,0\rangle$
E^-	$A_1\oplus A_4$	$[(56),E]$	$(E-E^*)(E-I_{ag})(E-I_g^*)\|0,0\rangle$
G_3^+	$E_2\oplus E_4$	$[E,-(23)(56),(56),-(23)]$	$(E+E^*)(E-I_g^*)\|1,-1\rangle$
G_3^+	$E_2\oplus E_4$	$[(56),(23),E,-(23)(56)]$	$(E+E^*)(E-I_{ag})\|1,1\rangle$
G_3^-	$E_1\oplus E_4$	$[E,-(23)(56),(56),-(23)]$	$(E-E^*)(E+I_g^*)\|1,-1\rangle$
G_3^-	$E_1\oplus E_4$	$[(56),-(23),E,(23)(56)]$	$(E-E^*)(E-I_{ag})\|1,1\rangle$
G_4^+	$E_1\oplus E_3$	$[E,(23)(56),(56),(23)]$	$(E+E^*)(E+I_g^*)\|1,-1\rangle$
G_4^+	$E_1\oplus E_3$	$[(56),(23),E,(23)(56)]$	$(E+E^*)(E+I_{ag})\|1,1\rangle$
G_4^-	$E_2\oplus E_3$	$[E,(23)(56),(56),(23)]$	$(E-E^*)(E-I_g^*)\|1,-1\rangle$
G_4^-	$E_2\oplus E_3$	$[(56),-(23),E,-(23)(56)]$	$(E-E^*)(E+I_{ag})\|1,1\rangle$
G_1^+	G	$[E,I_{ag},I_{ag}(23),(23)]$	$(E+E^*)[E+(56)]\|1,0\rangle$
G_1^-	G	$[E,I_{ag},-I_{ag}(23),-(23)]$	$(E-E^*)[E+(56)]\|1,0\rangle$
G_2^+	G	$[E,I_{ag},-I_{ag}(23),-(23)]$	$(E+E^*)[E-(56)]\|1,0\rangle$
G_2^-	G	$[E,I_{ag},I_{ag}(23),(23)]$	$(E-E^*)[E-(56)]\|1,0\rangle$

dimensional we must not forget the reordering by $\mathbb{T}$, see the Appendix) and if (56) maps onto a nonequivalent irrep we obtain a G_{144} irrep of double dimension. Thus, for instance, from $(A_1\otimes A_1)^+$ we obtain the A_1^+ and B_2^+ functions of Table V. The first set of E^- functions of Table V are spanned by $(A_1\otimes A_1)^-G_{72}$ functions and their images under (56), which transform as $(A_2\otimes A_2)^-$. The second set of E^- functions is spanned by $(A_2\otimes A_2)^-$ functions and their images under (56).

The functions derived from $E\otimes E=G$ require special attention because the matrices $\mathbb{D}^G(h_i^{ag}h_j^g)$ and $\mathbb{D}^G(h_j^{ag}h_i^g)$ are equivalent, but not identical. This is due to the ordering of the basis which carries this four-dimensional outer product irrep. In this four-dimensional case a permutation of the second and third basis function is required. Hence, absorbing the E^* of I_g^* into $E+E^*$, we find that the second function carrying G_1^+ is

$$
\begin{aligned}
&(E+E^*)[I_{ag}+(56)I_g^*]|1,0\rangle\\
&\quad=(E+E^*)(I_{ag}+(56)I_g)|1,0\rangle\\
&\quad=(E+E^*)[I_{ag}+I_{ag}(56)]|1,0\rangle\\
&\quad=I_{ag}(E+E^*)[E+(56)]|1,0\rangle.
\end{aligned}
$$

The third function of G_1^+ is obtained by using,

$$
\begin{aligned}
&(E+E^*)[I_g^*+(56)I_{ag}]\\
&\quad=(E+E^*)[(56)I_{ag}(56)+(56)I_{ag}]\\
&\quad=(E+E^*)(56)I_{ag}[(56)+E]\\
&\quad=(E+E^*)I_{ag}(23)[E+(56)].
\end{aligned}
$$

The first and fourth are simply obtained by projecting with $E+(56)$, where we notice that $I_{ag}I_g=(23)(56)$ and $(56)[E+(56)]=[E+(56)]$.

When we need to consider $A_2\otimes E$ in the case of odd parity functions, we must realize that this irrep is equivalent to E, but not identical to it. By our construction it follows that

$$
A_2\otimes\mathbb{D}^E=\begin{pmatrix}1&0\\0&-1\end{pmatrix}\mathbb{D}^E\begin{pmatrix}1&0\\0&-1\end{pmatrix}.
$$

When constructing bases for the G_1^- and G_2^- irreps, we must combine this transformation with the required reordering of the tensor product basis. Thus, $\pm(56)$ must act on $|1,0\rangle$, $-I_g^*|1,0\rangle$, $-I_{ag}|1,0\rangle$, and $I_{ag}I_g^*|1,0\rangle$, respectively. The remainder of Table V follows by similar reasoning.

We have shown that we only have to inspect four combinations of (k_A,k_B). These combinations can be operated on with the four generators I_{ag}, I_g^*, (56), E^*, and their products, yielding maximally sixteen linear independent functions per combination. For *ortho–ortho* dimers, $(k_A,k_B)=(0,0)$, this gives rise to all $A^\pm$, $B^\pm$, and $E^\pm$ functions of G_{144}. The *para–ortho* combination $(k_A,k_B)=(1,0)$ induces to $G_1^\pm$ or $G_2^\pm$ functions. Operation on *para–para* functions with $(k_A,k_B)=(1,1)$ yields one set of $G_3^\pm$ and $G_4^\pm$ functions and on functions with $(k_A,k_B)=(1,-1)$ yields the other. The total of 64 functions matches exactly the sixteen-dimensional space spanning all irreps of G_{36} times the four quadrants in Fig. 1.

By the construction outlined in this section the basis functions of G_{144} symmetry Γ, listed in Table V, are obtained by the action of operators $W_a^{\Gamma,\gamma}$ on functions adapted to γ of

G_{36}. These latter functions are listed in Table IV. The projectors adapt not only the basis, but also the van der Waals states which are obtained from this basis. That is, $W_a^{\Gamma,\gamma}|\psi_{a,i}^{\gamma},\sigma_A,\sigma_B\rangle$ is adapted to G_{144}. The operator $W_a^{\Gamma,\gamma}$ commutes with H, a fact that will give a drastic simplification in the calculation of matrix elements of H as will be shown in the next section. (A derivation of the results in Tables IV and V, which is conceptually simpler but more laborious, is through the use of the character projectors of G_{36} and G_{144}. This method gives less insight in the simultaneous adaptation of the wave functions to the group G_{144} and to its subgroup G_{36}, which is an essential element of this paper.)

III. ENERGY SPLITTINGS

In this section we will calculate the splittings by diagonalizing $H=H_{\rm vdw}+V$ on the zeroth-order functions described in Sec. II. Since several unperturbed levels are less than 1 cm^{-1} apart, one would expect that all of these have to be treated in a quasidegenerate manner. However, only two of these pairs interact in quasidegenerate first order. These are the $K=0$ pairs with symmetry E_1/E_3 and E_2/E_4. In these cases a problem of double dimension must be solved. Other nearly degenerate pairs are $|K|=1$ E_3/E_4, A_1/A_2, and A_3/A_4 states. Since it follows from Table V that E_3 of G_{36} induces to $G_4^{\pm}$ of G_{144} and E_4 to $G_3^{\pm}$, these states are noninteracting under the Hamiltonian H, which by definition transforms as A_1^+. Likewise, the nearly degenerate A_1/A_2 pair is noninteracting, because A_1 induces to $A_1^+\oplus B_2^+\oplus E^-$ and A_2 to $A_2^-\oplus B_1^-\oplus E^+$. Moreover, the nearly degenerate A_3/A_4 van der Waals states cannot mix for similar reasons.

By using the orthogonality $\langle\psi^+(\rho)|H_{\rm inv}|\psi^-(\rho)\rangle=0$ we can relate $\langle+|H_{\rm inv}|-\rangle$, needed in the calculations, to the monomer inversion splitting $\Delta=0.793$ cm^{-1} as

$$\begin{aligned}\langle+|H_{\rm inv}|-\rangle&\equiv\langle f_+(\rho)|H_{\rm inv}|f_-(\rho)\rangle\\&=\tfrac{1}{2}(\langle\psi^+|H_{\rm inv}|\psi^+\rangle-\langle\psi^-|H_{\rm inv}|\psi^-\rangle)\\&=\tfrac{1}{2}([E_0-\tfrac{1}{2}\Delta]-[E_0+\tfrac{1}{2}\Delta])\\&=-\tfrac{1}{2}\Delta,\end{aligned}$$

where $E_0=\langle+|H_{\rm inv}|+\rangle=\langle-|H_{\rm inv}|-\rangle$ is the energy of the lowest ν_2 mode.

We will exemplify the calculation of the matrix elements by first considering the G_{144} states that correlate with A_1 of G_{36}, i.e., the states of A_1^+, B_2^+, and E^- symmetry. From comparison of Tables IV and V we find that the first state, $W^{A_1^+,A_1}|\psi_i^{A_1},+,+\rangle$, is obtained by the projector $W^{A_1^+,A_1}=(E+E^*)[E+(56)]$. We find from Table IV that the VRT state $|\psi_i^{A_1}\rangle$ of energy $\mathscr{E}_i^{A_1}$ is

$$|\psi_i^{A_1}\rangle=\sum_{\{\Lambda\},n}{}'C^{A_1}_{\{\Lambda\},n;i}(E+I_{\rm ag})(E+I_g^*)|\{\Lambda\},J,M,n\rangle.$$

Here $\{\Lambda\}=\{j_A,k_A,j_B,k_B,j,K\}$ and $k_A,k_B=0$ (mod 3). Using

$$(W^{A_1^+,A_1})^2=4W^{A_1^+,A_1},\tag{3}$$

and

$$\begin{aligned}\langle\psi_i^{A_1}+,+|E^*|\psi_i^{A_1}+,+\rangle&=\langle\psi_i^{A_1}+,+|(56)|\psi_i^{A_1}+,+\rangle\\&=\langle\psi_i^{A_1}+,+|(56)^*|\psi_i^{A_1}+,+\rangle\\&=0,\end{aligned}$$

which follows from the symmetry operations in Table II, we obtain that the norm of the A_1^+ states is 2.

Using the Hermiticity of $W^{A_1^+,A_1}$, the fact that it commutes with the Hamiltonian, and Eq. (3), we get

$$\begin{aligned}E_i^{A_1^+}=\langle\psi_i^{A_1},+,+|&H_{\rm vdw}+H_{\rm inv}(\rho_A)\\&+H_{\rm inv}(\rho_B)|W^{A_1^+,A_1}\psi_i^{A_1},+,+\rangle.\end{aligned}$$

As we can see in Table II, E^* and (56) transform $|+,+\rangle$ into a ket orthogonal to it, so that only one term arises from $H_{\rm vdw}$, which is $\mathscr{E}_i^{A_1}$. The inversion $H_{\rm inv}(\rho_A)$ gives rise to two terms, one from the identity operator E, which gives the energy E_0 and one from (56)*, giving $-\frac{1}{2}\Delta$. Similarly, $H_{\rm inv}(\rho_B)$ gives only nonzero contributions when multiplied by E and (56). The zero-point energy $2E_0$ of the ν_2 vibrations of the two umbrellas will be taken as our reference energy and, thus, we find that

$$E_i^{A_1^+}=\mathscr{E}_i^{A_1}-\tfrac{1}{2}\langle\psi_i^{A_1}|(56)^*|\psi_i^{A_1}\rangle\Delta-\tfrac{1}{2}\langle\psi_i^{A_1}|(56)|\psi_i^{A_1}\rangle\Delta.$$

This can be simplified further by virtue of the A_1 symmetry of the zeroth-order state, namely,

$$\begin{aligned}(56)^*[E+I_{\rm ag}][E+I_g^*]&=(56)^*I_g^*[E+I_{\rm ag}][E+I_g^*]\\&=I_{\rm ag}(56)[E+I_{\rm ag}][E+I_g^*].\end{aligned}$$

Using the turnover rule on $I_{\rm ag}$, absorbing it into the bra, and using the orthonormality of the basis, we arrive at

$$\begin{aligned}E_i^{A_1^+}&=\mathscr{E}_i^{A_1}-\Delta\langle\psi_i^{A_1}|(56)|\psi_i^{A_1}\rangle\\&=\mathscr{E}_i^{A_1}-\Delta\sum_{\substack{\{\Lambda\},n\\\{\Lambda'\},n'}}c^{A_1}_{\{\Lambda\},n;i}c^{A_1}_{\{\Lambda'\},n';i}\\&\quad\times\langle\{\Lambda\},J,M,n|(56)|\{\Lambda'\},J,M,n'\rangle\\&=\mathscr{E}_i^{A_1}-\Delta\sum_{\{\Lambda\},n}(-1)^{j_B}c^{A_1}_{\{\Lambda\},n;i}c^{A_1}_{\{\tilde\Lambda\},n;i}\end{aligned}\tag{4}$$

with $\{\tilde\Lambda\}=\{j_A,k_A,j_B,-k_B,j,K\}$. The coefficients $c^{A_1}_{\{\Lambda\},n;i}$ are obtained from the six-dimensional VRT calculations described in the accompanying paper. In the very same way we compute

$$E_i^{B_2^+}=\mathscr{E}_i^{A_1}+\Delta\sum_{\{\Lambda\},n}(-1)^{j_B}c^{A_1}_{\{\Lambda\},n;i}c^{A_1}_{\{\tilde\Lambda\},n;i}.\tag{5}$$

The E^- irrep also correlates with A_1 of G_{36}. Looking into Table V, we find two E^- pairs. Since they carry identical matrix irreps, the first basis function of the one pair mixes only with the first of the other pair and not with the second of the other pair. These first basis functions are $(E-E^*)|\psi_i^{A_1},+,+\rangle$ and $(56)(E-E^*)|\psi_i^{A_4},+,+\rangle$, respectively. In principle, we would have to solve now a 2×2 secular problem on basis of these two functions. The

diagonal elements in this secular problem are $\mathscr{E}_i^{A_1}$ and $\mathscr{E}_i^{A_4}$, respectively, which differ by about 16 cm^{-1}. Since the off-diagonal element is $\Delta\langle\psi^{A_1}|(56)|\psi^{A_4}\rangle$, it is smaller than Δ and can be neglected with respect to the difference in diagonal elements. Therefore, we write

$$E_i^{E^-} = \mathscr{E}_i^{A_1}. \tag{6}$$

From Eqs. (4)–(6) we conclude that the zeroth-order A_1 state splits into four states: one higher in energy and one lower by the same amount, and two states (the degenerate E^- pair) unmoved.

We have shown how to compute the splittings due to monomer inversion by choosing the unperturbed A_1 state as an example. From the physical point of view this choice is not the most relevant, because both the A_1^+ and the E^- state have spin statistical weight zero for the protonated dimer.[5] Hence the splitting of the A_1 state is not observable for this isotopomer. The same remark applies to the other VRT states of A symmetry. This situation is comparable with the $k=0$ states in the free NH_3 monomer, where also one of the two components of each inversion doublet has weight zero and the splittings are not directly observable. Dimer states arising from G, however, do give rise to observable splittings, since G induces to $G_1^+ \oplus G_1^- \oplus G_2^+ \oplus G_2^-$, and the latter two irreps have nonzero spin statistical weight, whereas the former are Pauli forbidden in the protonated dimer. By the same kind of manipulations as for the A_1 states, we derive from the first $G_2^\pm$ functions of Table V

$$E_i^{G_2^+} = \mathscr{E}_i^G + \tfrac{1}{2}\Delta\langle\psi_i^G|(56)|\psi_i^G\rangle + \tfrac{1}{2}\Delta\langle\psi_i^G|(56)^*|\psi_i^G\rangle,$$

$$E_i^{G_2^-} = \mathscr{E}_i^G + \tfrac{1}{2}\Delta\langle\psi_i^G|(56)|\psi_i^G\rangle - \tfrac{1}{2}\Delta\langle\psi_i^G|(56)^*|\psi_i^G\rangle.$$

We cannot eliminate (56)* here, because in this case we are describing different monomers: *ortho* $[k=0 \pmod 3]$ and *para* $[k=1 \pmod 3]$. From Table II we deduce that (56)* flips the *para* umbrella. We also observe in Table II that (56)* inverts the sign of K, and since states with different K are orthogonal, it follows that our model predicts an observable splitting of the G states only in the case of $K=0$ (as long as one neglects the Coriolis interactions). The matrix elements of (56) and (56)* are again simply related to the coefficient vectors obtained from the VRT calculations. In the fully deuterated dimer the $G_1^\pm$ states are Pauli allowed as well. The splitting between these states and the $G_2^\pm$ states are due to inversion of the *ortho* umbrella. Since this inversion is caused by the permutation (56) and since this permutation leaves K invariant, the corresponding splitting should be significant also in the states with $K\neq 0$.

We next turn to the quasidegenerate E_1/E_3 pairs for $K=0$ and even J. We can read off from Table V that $E_1\uparrow G_{144} = G_3^- \oplus G_4^+$ and $E_3\uparrow G_{144} = G_4^- \oplus G_4^+$. The states G_3^- and G_4^- are unaffected in first order and accordingly will have the energies of E_1 and E_3, respectively. The G_4^+ contents of both states will mix in quasi first order, however, and this gives rise to a splitting. We solve a secular problem on basis of

$$(E+E^*)|\psi^{E_1},+,+\rangle \quad \text{and} \quad (56)(E+E^*)|\psi^{E_3},+,+\rangle,$$

where, in the symbolic shorthand notation of Table IV, $|\psi^{E_1}, +, +\rangle$ is expanded in terms of $(E + I_g^*)|1,-1\rangle$ and $|\psi^{E_3}, +, +\rangle$ in terms of $(E+I_{ag})|1,1\rangle$. We obtain the following H matrix

$$\begin{pmatrix} \mathscr{E}^{E_1} & -\langle\psi^{E_1}|(56)|\psi^{E_3}\rangle\Delta \\ -\langle\psi^{E_3}|(56)|\psi^{E_1}\rangle\Delta & \mathscr{E}^{E_3} \end{pmatrix},$$

with eigenvalues

$$E_\pm^{G_4^+} = \tfrac{1}{2}(\mathscr{E}^{E_1} + \mathscr{E}^{E_3}) \pm [\langle\psi^{E_3}|(56)|\psi^{E_1}\rangle^2\Delta^2 + \tfrac{1}{4}(\mathscr{E}^{E_1} - \mathscr{E}^{E_3})^2]^{1/2},$$

which again are easily computed, since the VRT states ψ^{E_1} and ψ^{E_3} and their energies $\mathscr{E}^{E_1}$ and $\mathscr{E}^{E_3}$ are known. In summary, we find that the E_1/E_3 pairs give rise to $G_4^+, G_4^-, G_3^-, G_4^+$. In our quasi-first-order model only the G_4^+ states are split. The G_3^- and G_4^- states are unaffected and have the energies of the original E_3 and E_1 levels, respectively. In the discussion of the numerical results, we will see that these levels correspond to the measured levels labeled (1) to (4) in Fig. 3(a) of Ref. 5 and in Table VI of our accompanying paper.[7]

The development for the quasidegenerate E_2/E_4 pairs runs completely analogous: since $E_2\uparrow G_{144} = G_3^+ \oplus G_4^-$ and $E_4\uparrow G_{144} = G_3^+ \oplus G_3^-$, the G_4^- and G_3^- states are not shifted, and two G_3^+ states arise, with energies

$$E_\pm^{G_3^+} = \tfrac{1}{2}(\mathscr{E}^{E_2} + \mathscr{E}^{E_4}) \pm [\langle\psi^{E_2}|(56)|\psi^{E_4}\rangle^2\Delta^2 + \tfrac{1}{4}(\mathscr{E}^{E_2} - \mathscr{E}^{E_4})^2]^{1/2}.$$

In Table VI all the splittings are summarized, together with the spin statistical weights of the levels. The latter can be found by application of the $G_{36}\subset G_{144}$ induction procedure outlined in Sec. II to the nuclear spin functions in Table VII of Ref. 11. For odd J the states E_3 and E_4 change roles. The pairs E_1/E_4 and E_2/E_3 are nearly degenerate for $K=0$ and the mixing occurs in G_3^- and G_4^-. The energies belonging to these irreps are

$$E_\pm^{G_3^-} = \tfrac{1}{2}(\mathscr{E}^{E_1} + \mathscr{E}^{E_4}) \pm [\langle\psi^{E_1}|(56)|\psi^{E_4}\rangle^2\Delta^2 + \tfrac{1}{4}(\mathscr{E}^{E_1} - \mathscr{E}^{E_4})^2]^{1/2}.$$

and

$$E_\pm^{G_4^-} = \tfrac{1}{2}(\mathscr{E}^{E_2} + \mathscr{E}^{E_3}) \pm [\langle\psi^{E_2}|(56)|\psi^{E_3}\rangle^2\Delta^2 + \tfrac{1}{4}(\mathscr{E}^{E_2} - \mathscr{E}^{E_3})^2]^{1/2},$$

respectively.

IV. RESULTS: COMPARISON WITH EXPERIMENT

With the use of the model and the formulas derived in Secs. II and III, we have calculated the umbrella inversion splittings in both $(NH_3)_2$ and $(ND_3)_2$. The six-dimensional bound state wave functions $\psi_{a,i}^\gamma$ were obtained from several different potentials, which have different barriers for the interchange of the proton donor and the acceptor in the hydrogen bond and for the rotations of the monomers about their C_3 axes. In the potential of Sagarik *et al.*,[17] which was used

TABLE VI. Energies of G_{144} states affected by inversion splitting. The spin statistical weights are w_H in $(NH_3)_2$ and w_D in $(ND_3)_2$. This table applies to even J; for odd J one has to swap the irrep labels $E_3 \leftrightarrow E_4$ and $G_4^+ \leftrightarrow G_3^\mp$ and the corresponding weights.

w_H	w_D	Energy expression
0	465	$E^{A_1^+} = \mathscr{E}^{A_1} - \Delta\langle\psi^{A_1}\|(56)\|\psi^{A_1}\rangle$
66	6	$E^{B_2^+} = \mathscr{E}^{A_1} + \Delta\langle\psi^{A_1}\|(56)\|\psi^{A_1}\rangle$
0	90	$E^{E^-} = \mathscr{E}^{A_1}$
78	3	$E^{A_2^-} = \mathscr{E}^{A_2} + \Delta\langle\psi^{A_2}\|(56)\|\psi^{A_2}\rangle$
0	435	$E^{B_1^-} = \mathscr{E}^{A_2} - \Delta\langle\psi^{A_2}\|(56)\|\psi^{A_2}\rangle$
0	90	$E^{E^+} = \mathscr{E}^{A_2}$
0	465	$E^{A_1^-} = \mathscr{E}^{A_3} - \Delta\langle\psi^{A_3}\|(56)\|\psi^{A_3}\rangle$
66	6	$E^{B_2^-} = \mathscr{E}^{A_3} + \Delta\langle\psi^{A_3}\|(56)\|\psi^{A_3}\rangle$
0	90	$E^{E^+} = \mathscr{E}^{A_3}$
78	3	$E^{A_2^+} = \mathscr{E}^{A_4} + \Delta\langle\psi^{A_4}\|(56)\|\psi^{A_4}\rangle$
0	435	$E^{B_1^+} = \mathscr{E}^{A_4} - \Delta\langle\psi^{A_4}\|(56)\|\psi^{A_4}\rangle$
0	90	$E^{E^-} = \mathscr{E}^{A_4}$
21	276	$E^{G_3^+} = \frac{1}{2}(\mathscr{E}^{E_2} + \mathscr{E}^{E_4}) \pm [\Delta^2\langle\psi^{E_2}\|(56)\|\psi^{E_4}\rangle^2 + \frac{1}{4}(\mathscr{E}^{E_2} - \mathscr{E}^{E_4})^2]^{1/2}$
21	276	$E^{G_3^-} = \mathscr{E}^{E_1}$
21	276	$E^{G_3} = \mathscr{E}^{E_4}$
15	300	$E^{G_4^+} = \frac{1}{2}(\mathscr{E}^{E_1} + \mathscr{E}^{E_3}) \pm [\Delta^2\langle\psi^{E_1}\|(56)\|\psi^{E_3}\rangle^2 + \frac{1}{4}(\mathscr{E}^{E_1} - \mathscr{E}^{E_3})^2]^{1/2}$
15	300	$E^{G_4^-} = \mathscr{E}^{E_2}$
15	300	$E^{G_4} = \mathscr{E}^{E_3}$
0	720	$E^{G_1^+} = \mathscr{E}^G - \frac{1}{2}\Delta\langle\psi^G\|(56)\|\psi^G\rangle - \frac{1}{2}\Delta\langle\psi^G\|(56)^*\|\psi^G\rangle$
0	720	$E^{G_1^-} = \mathscr{E}^G - \frac{1}{2}\Delta\langle\psi^G\|(56)\|\psi^G\rangle + \frac{1}{2}\Delta\langle\psi^G\|(56)^*\|\psi^G\rangle$
72	72	$E^{G_2^+} = \mathscr{E}^G + \frac{1}{2}\Delta\langle\psi^G\|(56)\|\psi^G\rangle + \frac{1}{2}\Delta\langle\psi^G\|(56)^*\|\psi^G\rangle$
72	72	$E^{G_2^-} = \mathscr{E}^G + \frac{1}{2}\Delta\langle\psi^G\|(56)\|\psi^G\rangle - \frac{1}{2}\Delta\langle\psi^G\|(56)^*\|\psi^G\rangle$

in Ref. 11, the interchange barrier is about 80 cm^{-1}, in the model potentials I,II,III,IV introduced in Refs. 18 and 19 this barrier varies between 0 and 30 cm^{-1}, and in the potential found in the preceding paper[7] it is 7 cm^{-1}. The latter potential yields van der Waals energy levels in perfect agreement with the far-infrared spectrum of $(NH_3)_2$.[5] The dipole moment and the nuclear quadrupole splittings of $(NH_3)_2$ and $(ND_3)_2$ calculated from the corresponding wave functions agree well with the values obtained by microwave spectroscopy.[4,20,21] In the detailed far-infrared and microwave study of Loeser *et al.*[5] the inversion splittings in $(NH_3)_2$ were explicitly measured. Obviously (see Sec. III), no splittings could be observed in the *ortho–ortho* states (A_1,A_2,A_3,A_4 in G_{36}). Inversion splittings of the order of a few GHz were found for the *ortho–para* states (the G states in G_{36}) and for the *para–para* states (E_1,E_2,E_3,E_4), but only for $K=0$. The splittings in the corresponding states with $K\neq 0$ are smaller by a few orders of magnitude.

Let us first discuss the G-state splittings for $K=0$, since these arise directly from the simple first-order model (see Sec. III). For all the potentials used to calculate the bound van der Waals states, it appears that in the lowest G state with $K=0$ the *para*-NH_3 monomer is the proton donor and the *ortho* monomer is the proton acceptor. This holds even when the equilibrium structure has the cyclic geometry with two equivalent monomers, and the inequivalence of the monomers is imposed only by the *ortho–para* difference. In the first excited G state the situation is reversed: The *para* monomer is the proton acceptor. It follows from Sec. III that it is only the inversion of the *para* monomer which leads to an observable splitting in the protonated dimer. Every G level splits into a $G_2^\mp$ doublet. If we look at the experimental data in Table VII we observe that, for both monomers, the umbrella inversion in $(NH_3)_2$ is about 10 times slower than in the free monomer. Combining calculations and experiment we conclude, since the excited G state splits less than the ground state, that the inversion of the proton acceptor is more strongly hindered than that of the donor. This might have been expected from geometric considerations, which are most evident when we look at a structure with a linear hydrogen bond. The calculations with the potential from the preceding paper[7] give nearly correct splittings, see Table VII. With the potential of Sagarik *et al.*[17] used in the earlier calculations[11] this is not the case: The ground state splitting is then 1.67 GHz, which is reasonable, but the excited G-state splitting is 0.09 GHz, which is too small by a factor of 25. This reflects the fact that with this potential even the average structure has a nearly linear hydrogen bond and the proton acceptor, with its lone pair almost parallel to the bond axis, is difficult to invert. With the different model potentials I–IV introduced in Refs. 18 and 19, the calculated inversion splittings vary by more than a factor of 2 see, e.g., Table IV of Ref. 18. The fact that we now obtain inversion splittings which are nearly correct, both absolutely and relatively, in-

TABLE VII. Inversion splittings in $(NH_3)_2$, with the free monomer value $\Delta=23.79$ GHz (Ref. 13) and with the optimized value $\Delta=41.52$ GHz.

		Calculation		
	State labels[a]	$\Delta=23.79$	41.52 Ghz	Experiment (Ref. 5)
		$J=K=0$		
$G_2^+-G_2^-$	(2)-(1)	2.052	3.581 GHz	3.309 GHz
$G_2^+-G_2^-$	(12)-(11)	1.235	2.155 GHz	2.392 GHz
$\Delta\langle\psi^{E_1}\|(56)\|\psi^{E_3}\rangle$[b]	(4)/(1)	0.769	1.342 GHz	1.182 GHz
$\Delta\langle\psi^{E_2}\|(56)\|\psi^{E_4}\rangle$[c]	(16)/(13)	1.621	2.829 GHz	2.871 GHz
		$J=1$, $K=\pm1$		
$G_4^+-G_4^-$[d]	(9)-(7)	12.3	37.7 MHz	48.3 MHz
$G_3^--G_3^+$[d]	(10)-(8)	12.3	37.7 MHz	47.7 MHz
$G_2^--G_2^+$	(4)-(3)	1.15	2.0 MHz	2.0 MHz
$G_2^--G_2^+$	(5)-(6)	−0.82	−1.4 MHz	−0.6 MHz
$G_2^--G_2^+$[e]	(10)-(9)	11.85	20.7 MHz	32.7 MHz
$G_2^--G_2^+$	(14)-(13)	0.35	0.6 MHz	0.1 MHz

[a]State labels as in Fig. 3 and Table IV of Ref. 5; the $G_3^\pm$ and $G_4^\pm$ states as in Table IV(a) and the $G_2^\pm$ states as in Table IV(b). Note that the (arbitrary) parity assignment of the $G_2^\pm$ levels in Ref. 5 is reversed here.
[b]Off-diagonal matrix element between states of G_4^+ symmetry.
[c]Off-diagonal matrix element between states of G_3^+ symmetry.
[d]From mixing with lower G_4^+/G_3^- levels (see Fig. 3).
[e]Note the strong Coriolis coupling with the $J=1$, $K=0$ states labeled (11,12).

dicates that the potential found in the preceding paper[7] is indeed realistic.

The far-infrared spectrum determines only the relative parity of the levels, not the absolute overall parity. In Ref. 5 it was arbitrarily assumed that the lowest of the $G_2^\pm$ levels with $K=0$ has G_2^+ symmetry. It follows from our results that this parity assignment must be reversed. The remaining discrepancy with the experimental values may be caused by the changes in the intramonomer barrier for inversion, induced by the interaction with the other monomer. This is not taken into account by the present model, as long as we take the splitting parameter Δ from the free monomer. Remember that the interactions in $(NH_3)_2$ are much stronger than in Ar–NH_3, for which the model proved to work very precisely.[8] We can include (in a rather crude manner) the effect of these interactions on the monomer inversion barriers by introducing an effective value of Δ into our model. A best fit (in the least-squares sense) of the splittings in the G states with $K=0$ yields a value of Δ which is larger than the monomer value by a factor of 1.75 (see Table VII). We performed a few simple calculations on the free NH_3 monomer and found that this factor of 1.75 in Δ corresponds to a 9% decrease of the height of the inversion barrier.

Next we consider the G states with $K=\pm1$ and $K=\pm2$. If we neglect the off-diagonal Coriolis coupling and assume that K is a good quantum number for the bound van der Waals states, then it follows from Secs. II and III that in the protonated dimer no splitting of these states should be observed. Experimentally, these $G_2^\pm$ splittings are indeed very small, see Table VII. The splittings observed in the $K=\pm1$ states can be understood if we realize that they are caused by the Coriolis mixing with the $K=0$ states: they "steal" the inversion splittings from the latter states. The amount of Coriolis mixing depends on the energy differences between the unperturbed states with $K=\pm1$ and those with $K=0$. Especially the excited state with $K=1$ which corresponds to the labels (9,10) in Table VI of our accompanying paper,[7] mixes with the first excited $K=0$ state, i.e., the state labeled (11,12), since these states are nearly degenerate. We observe in Table VII that, indeed, the splitting of this state (32.7 MHz) is considerably larger than that of the other $K=\pm1$ states.

In the final stage of our calculations in the preceding paper[7] the Coriolis mixing was explicitly included. It was calculated by diagonalizing the matrix of the Hamiltonian including the Coriolis coupling, in a basis of eigenstates which were obtained without Coriolis coupling (for which K is a good quantum number). In this basis we included the lowest ten eigenstates for each value of K: -1, 0, and 1. The resulting eigenfunctions were then substituted into the formulas of Table VI. The effect of the Coriolis mixing on the inversion splittings is mostly very small, both absolutely and relatively. For the G states with $K=\pm1$, which would not be split without this Coriolis mixing, the calculated inversion splittings are listed in Table VII. We observe that even these small splittings agree well with the measured values, especially when we use the optimized value of Δ. Indeed, the (10)-(9) splitting is by far the largest.

In general, the order of the (calculated and measured) $G_2^\pm$ doublets, i.e., the sign of the splitting parameter, for $K=\pm1$ and $J=1$ is reversed with respect to that of the $J=K=0$ levels. The explanation that the G states with $K=\pm1$ obtain their inversion splitting only by "stealing" it from the G states with $K=0$ (via Coriolis mixing) leads to the same sign of the "internal" splitting parameter. The reversed order is caused by the rotational phase factor $(-1)^J$ which occurs when the umbrella inversion operator $(56)^*$ acts on the basis functions, see Table II. It is the action of this operator which splits the G levels into the G_2^+ and G_2^- components, see Table VI, by inversion of the para monomer. Thus, the G_2^- levels are lower for $J=K=0$ and the G_2^+ levels are lower for $J=1$, both for $K=0$ and for $K=\pm1$. Only the

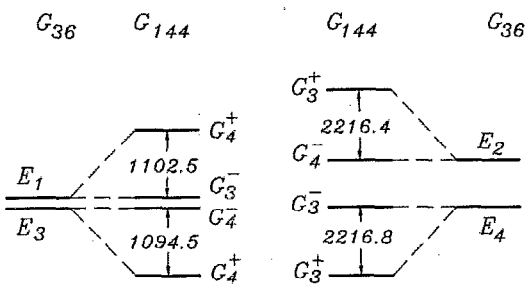

FIG. 2. Splitting by monomer umbrella inversion of the $K=0$ VRT *para–para* states. The splittings (in MHz) indicated are from experiment (Ref. 5). The states on the left-hand side have the labels (1)–(4) in Fig. 3(a) of Ref. 5 and in Table VI of Ref. 7, the states on the right-hand side are labeled (13)–(16). Our model predicts that the E_1/E_3 and E_2/E_4 levels split symmetrically. Observe that this holds experimentally to a very good approximation.

$K=-1$ levels (5,6) deviate from this rule, see Table VII. It turns out that the splitting between these levels is dominated by matrix elements of the operator (56)* between the $K=-1$ and the $K=1$ components (which interact through the $K=0$ states), rather than by the admixed $K=0$ components themselves. The latter contribute +0.2 MHz to the splitting between the levels (5) and (6), while the contribution from the $K=-1$ and $K=1$ mixing is −1.6 MHz (for the optimized value of Δ). Note that the G levels (5,6) with $K=-1$ are relatively close to the levels (3,4) with $K=1$. It is remarkable that the negative sign of this minute splitting between the levels (5) and (6) is given correctly by our calculations.

This explanation of the inversion splitting of the G states is confirmed by the observed J dependence of these splittings. For the G states with $K=0$ they are almost independent of J. The splittings of the $K=\pm1$ states, which we interpret as being introduced via the Coriolis mixing, are proportional to $J(J+1)$. The splittings of the G states with $K=\pm2$ are unobservably small.[5] This also is consistent with our explanation, since one needs indirect Coriolis mixing, via the states with $K=\pm1$ to the $K=0$ states, in order to obtain any inversion splitting of the $K=\pm2$ states.

Let us now discuss the splittings of the E_i states ($i=1,2,3,4$), first for $K=0$. The theory tells us that no pure first order splittings occur in these states. This follows from the adaptation of the E_i states to the G_{144} symmetry of the inverting dimer. The resulting $G_3^{\pm}$ and $G_4^{\pm}$ states are generated by the projector $(E\pm E^*)$, see Table V, and E^* inverts *both* monomers simultaneously, see Table II. In our model, with the perturbation $H_{\rm inv}(\rho_A)+H_{\rm inv}(\rho_B)$, this simultaneous inversion does not lead to an observable splitting. Still, the splittings observed[5] for the E_i states with $K=0$ are of the same order of magnitude as those of the G states. This is shown in Fig. 2, where it is also clarified how these splittings can be interpreted. It is important to realize that for $K=0$ the E_1 state is nearly degenerate with the E_3 state, and the E_2 state with the E_4 state. This is a rather surprising phenomenon, since the E_1-E_3 and E_2-E_4 splittings are caused by the anisotropy of the intermolecular potential, which is considerable. The calculations in the preceding paper[7] give nearly correct small splittings, however, and it is explained why these near degeneracies occur. However, given these small energy gaps, it is easy to mix the E_1 and E_3 states, as well as the E_2 and E_4 states. We include such mixing in our quasidegenerate first-order model. The symmetry aspects are relevant: only the G_4^+ component that arises from the E_1 state will mix with the corresponding component of the E_3 state (for even J). Similarly, the G_3^+ component of the E_2 state mixes with the corresponding component of the E_4 state. The other components remain unaffected, since they have different symmetries, see Table V and Fig. 2. As the amount of mixing (and splitting) depends very sensitively on the energy gaps between the unperturbed E_1/E_3 and E_2/E_4 states, and it is practically impossible to reproduce these (very small) gaps quantitatively by the bound state calculations, we have chosen to compare the off-diagonal umbrella-tunneling matrix elements, rather than the final splittings. These can be extracted from the experimental data[5] if one assumes that the perturbed E_i levels are given by the expressions in Table V. It follows from the measured values that this is indeed realistic: the $G_4^- - G_4^+$ splitting of the E_3 state nearly equals the $G_4^+ - G_3^-$ splitting of the E_1 state and the $G_3^- - G_3^+$ splitting of the E_4 state nearly equals the $G_3^+ - G_4^-$ splitting of the E_2 state, see Fig. 2. In Table VII we observe that the tunneling matrix elements calculated with the bound state wave functions and the potential from the preceding paper[7] agree well with the values extracted from experiment,[5] also for the E_i states.

Finally, we consider the E_i states ($i=1,2,3,4$) with $K=\pm1$. The inversion splittings observed for these states are somewhat larger than the splittings of the G states with $K=\pm1$, but much smaller than the splittings of the E_i states with $K=0$. We will now show that the mechanism which splits the E_i states with $K=\pm1$ is essentially the same as for the E_i states with $K=0$. The resulting splittings are considerably smaller, however, because the near degeneracies of the latter states do not occur for $K=\pm1$. It follows from our calculations that the off-diagonal umbrella-tunneling matrix elements are of similar size, but the energy gaps between the unperturbed states are much larger. Instead of the first-order approach for quasidegenerate states, one may now apply a second order perturbation formula to calculate the splittings. Another relevant observation is that the E_1 states with $K=\pm1$ do not split because the coupling of their G_3^- component with the corresponding component of the E_3 states is practically equal to the coupling of their G_4^+ component with the corresponding component of the E_4 states (see Fig. 3). This follows from the fact that the E_3 and E_4 levels with $|K|=1$ are degenerate (apart from a small Coriolis splitting), and that also their eigenvectors are (practically) the same. (One of the components in their symmetry projectors has a different sign, of course (see Table IV), but this does not affect the size of the coupling matrix elements). Thus, the observed[5] splitting pattern can be completely understood, see Fig. 3. The same reasoning holds for the G_3^+ and G_4^- components of the E_2 states with $K=\pm1$, which are not split either, but which contribute to the splitting of the nearby E_3 and E_4 states. Even the calculated size of the inversion splitting (37.7 MHz with the optimized value of Δ) of the lowest E_3 and E_4 states agrees well with the observed splittings,

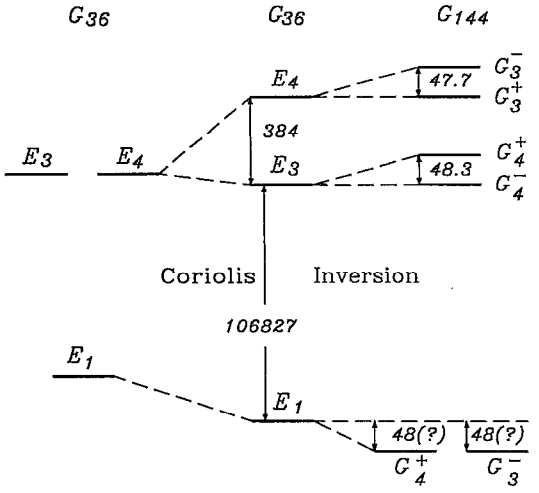

FIG. 3. Splitting of the $K=\pm 1$ VRT *para–para* states, first by Coriolis interaction and then by monomer inversions. Splittings indicated (in MHz) are from Ref. 5. The levels in this figure correspond to the states (5)–(10) in Fig. 3(a) of Ref. 5 and in Table VI of Ref. 7. The E_1 state does not split under inversion, since the interactions of its G_4^+ and G_3^- components with the E_3 and E_4 states, respectively, are as good as equal. We predict its shift to be of the same magnitude as the observed splittings, ca. 48 MHz.

which are indeed nearly equal (48.3 and 47.7 MHz). These splittings, by contrast with the Coriolis splitting between the E_3 and E_4 states with $|K|=1$ (384 MHz for the lowest pair, for $J=1$), are (almost) J independent. This is in accord with our interpretation.

V. CONCLUSION

The theory and the calculations presented in this paper lead to a detailed understanding of the observed umbrella inversion splittings in $(NH_3)_2$. We recall that these splittings, for the states with different symmetry and different K, range over 3 orders of magnitude. The calculated splittings are in quantitative agreement with the measured data.[5] The largest splittings occur for the mixed *ortho–para* states (the G states) with $K=0$, because these splittings originate from the inversion tunneling of the *para* monomer by a true first-order mechanism. Although this mechanism is absent for the *para–para* states (i.e., the states of E_1, E_2, E_3, and E_4 symmetry), the E_i levels with $K=0$ are split by almost equally large amounts. This is shown to be related to the near degeneracies in these levels, which lead to a quasi-first-order tunneling mechanism. It is essential in this mechanism that the different E_i states have components with the same G_{144} symmetry. For $K\neq 0$ the energy gaps between the unperturbed states of E_i symmetry are much larger, and the quasi-first-order mechanism becomes a second order effect. This explains why the splittings of the E_i states with $K\neq 0$ are considerably smaller. The very small splittings of the G states with $K=\pm 1$ are induced by an indirect mechanism, through Coriolis coupling. The "effective" value of Δ, which was optimized for the G states with $K=0$, considerably improves the results for all the other states too (see Table VII).

TABLE VIII. Inversion splittings in $(ND_3)_2$, $\Delta=1.600$ GHz (Ref. 13).

	Calculation
$J=K=0$	
$B_2^+-A_1^{+a}$	36.99 MHz
$B_2^+-A_1^{+b}$	56.76 MHz
$A_2^+-B_1^{+c}$	70.56 MHz
$A_2^+-B_1^{+d}$	−6.50 MHz
$G_2^+-G_2^{-e}$	50.29 MHz
$G_2^+-G_1^{-e}$	13.59 MHz
$G_2^+-G_2^{-f}$	58.93 MHz
$G_2^+-G_1^{-f}$	61.86 MHz
$\Delta\langle\psi^{E_1}\|(56)\|\psi^{E_3}\rangle^g$	21.13 MHz
$\Delta\langle\psi^{E_2}\|(56)\|\psi^{E_4}\rangle^h$	56.31 MHz

[a]Ground A_1 state.
[b]First excited A_1 state.
[c]Ground A_4 state.
[d]First excited A_4 state.
[e]Ground G state.
[f]First excited G state.
[g]Off-diagonal matrix element between states of G_4^+ symmetry.
[h]Off-diagonal matrix element between states of G_3^+ symmetry.

Since the inversion splittings appear to depend sensitively on the intermolecular potential used to generate the bound state wave functions, it is confirmed that the potential found in the preceding paper[7] is realistic. The umbrella inversion splittings calculated for $(ND_3)_2$ with the same potential are given in Table VIII. For Δ we have taken the value of 1.600 GHz for the free ND_3 monomer,[14] but, if the monomer inversion barriers are lowered by 9% [as we assumed when scaling Δ by a factor of 1.75 for $(NH_3)_2$], the splittings in $(ND_3)_2$ should be scaled by a factor of 2.1. The inversion splittings of the A_1, A_2, A_3, A_4 states and the splittings between the $G_1^{\pm}$ and $G_2^{\pm}$ components arising from the G states are also observable in this case. The theory predicts that these splittings will be relatively large and J independent, even for $K\neq 0$. In an absolute sense, however, the umbrella inversion splitting in ND_3 is considerably smaller than in NH_3, and the reduction of this splitting in the dimer is greater (see Table VIII). The predicted splittings are nevertheless sufficiently large to be measurable; we expect that they will soon be observed.

ACKNOWLEDGMENTS

This study was initiated while A. van der Avoird was a visiting Miller Research Professor at the University of California in Berkeley. He thanks the Miller Institute for Basic Research in Science for supporting this Professorship. J.L. and R.J.S. are supported by the National Science Foundation (Grant No. CHE-9123335).

APPENDIX

It is well known that the irreducible representations (irreps) of an outer direct product group are Kronecker products of the irreps of the factors. Since the corresponding result for semidirect products is more involved[16] and less well known, we review briefly how to construct an irrep Γ of an arbitrary group $G\equiv H(\mathbb{S})\{e,s\}$, from the irrep $\mathbb{D}(h)^\gamma$ of H. Let $\psi^\gamma=(\psi_1^\gamma,\ldots,\psi_{f_\gamma}^\gamma)$ carry the f_γ-dimensional irrep $\mathbb{D}(h)^\gamma$,

$$h\psi^{\gamma}=\psi^{\gamma}\mathbb{D}(h)^{\gamma}, \quad h\in H.$$

Since by the definition of a semidirect product the subgroup H is invariant in G, we have $hs=sh'$ with $h'\in H$. Acting with the element $h(e\pm s)$, we find

$$h(e\pm s)\psi^{\gamma}=\psi^{\gamma}\mathbb{D}(h)^{\gamma}\pm s\psi^{\gamma}\mathbb{D}(h')^{\gamma}, \quad h,h'\in H.$$

If $\mathbb{D}(h)^{\gamma}=\mathbb{D}(s^{-1}hs)^{\gamma}=\mathbb{D}(h')^{\gamma}$ for all $h\in H$, then it is clear that $(e\pm s)\psi^{\gamma}$ carries an irrep of G, where the elements of the coset Hs are represented by $\pm\mathbb{D}^{\gamma}$, because $hs(e\pm s)=\pm h(e\pm s)$. If $\mathbb{D}(h)^{\gamma}$ and $\mathbb{D}(s^{-1}hs)^{\gamma}$ are equivalent, but not identical, we find by an easy extension of the argument that also an f_{γ}-dimensional irrep of G is generated, but carried by the basis $(\psi^{\gamma}\pm s\psi^{\gamma}\mathbb{T})$, where $\mathbb{T}$ gives the equivalence transformation.

If, on the other hand, we assume that $\mathbb{D}(h)^{\gamma}$ and $\mathbb{D}(h')^{\gamma}=\mathbb{D}(s^{-1}hs)^{\gamma}=\mathbb{D}(h)^{\gamma'}$, while γ and γ' are nonequivalent irreps, then

$$h(\psi^{\gamma},s\psi^{\gamma})=(\psi^{\gamma},s\psi^{\gamma})\begin{pmatrix}\mathbb{D}(h)^{\gamma} & 0\\ 0 & \mathbb{D}(h)^{\gamma'}\end{pmatrix}$$

and

$$hs(\psi^{\gamma},s\psi^{\gamma})=(\psi^{\gamma},s\psi^{\gamma})\begin{pmatrix}0 & \mathbb{D}(h)^{\gamma}\\ \mathbb{D}(h)^{\gamma'} & 0\end{pmatrix}.$$

By Schur's lemma it is possible to reduce such a set of matrices if and only if γ and γ' are equivalent, which by assumption is not the case. Hence, a $2f_{\gamma}$-dimensional irrep of G is obtained, which is carried by $(\psi^{\gamma},s\psi^{\gamma})$. It is evident that this construction yields a sequence adapted basis, i.e., restriction of the irrep of G to H gives a decomposed irrep. It is of interest to relate this group structure to the Wigner operators, defined by

$$P^{\Gamma}_{ab}=\sum_{g\in G}D(g^{-1})^{\Gamma}_{ba}g.$$

In the first case, when the restriction of Γ to H is γ, it is easily shown that

$$P^{\Gamma}_{ab}=(e\pm s)Q^{\gamma}_{ab},$$

where Q^{γ}_{ab} is a Wigner operator for H. In the second case, where $\Gamma\downarrow H=\gamma\oplus\gamma'$, the subscripts are compound indices: $a\mapsto(\lambda,a')$ and $b\mapsto(\mu,b')$, and

$$P^{\Gamma}_{\lambda,a';\mu,b'}=\begin{cases}Q^{\gamma}_{a'b'} & \text{for } \lambda=\mu\\ sQ^{\gamma}_{a'b'} & \text{otherwise}\end{cases}.$$

It follows that $P^{\Gamma}_{ab}=W^{\Gamma,\gamma}Q^{\gamma}_{a'b'}$ with $W^{\Gamma,\gamma}=(e\pm s)$, e, or s. We have to repeat this procedure several times, when going along the group chain, and it is clear that $W^{\Gamma,\gamma}$ will be a simple product of coset generators and factors of the $e\pm s$ kind. Another group theoretical fact needed in the development of the main text is the following. Consider two commuting isomorphic groups H and H' with $h_i\leftrightarrow h'_i$, $h_i\in H$, $h'_i\in H'$, and $i=1,\ldots,|H|=|H'|$. Let $H\otimes H'\subset G$ and let $s\in G$ be such that $h_ih'_js=sh_jh'_i$, i.e., $(H\otimes H')\circledS\{e,s\}$ is a wreath product.[22,23] Suppose further that the groups have identical—not just equivalent—irreps, i.e., $\mathbb{D}(h_i)^{\gamma}=\mathbb{D}(h'_i)^{\gamma}$ for all γ and i. If

$$h_ih'_j\psi^{\gamma}\otimes\phi^{\gamma'}=\psi^{\gamma}\otimes\phi^{\gamma'}\mathbb{D}(h_i)^{\gamma}\otimes\mathbb{D}(h'_j)^{\gamma'},$$

then, using that the irreps are identical, we find

$$\begin{aligned}h_ih'_js\psi^{\gamma}\otimes\phi^{\gamma'}&=sh_jh'_i\psi^{\gamma}\otimes\phi^{\gamma'}\\&=s\psi^{\gamma}\otimes\phi^{\gamma'}\mathbb{D}(h_j)^{\gamma}\otimes\mathbb{D}(h'_i)^{\gamma'}\\&=s\psi^{\gamma}\otimes\phi^{\gamma'}\mathbb{D}(h'_j)^{\gamma}\otimes\mathbb{D}(h_i)^{\gamma'}\\&=s\psi^{\gamma}\otimes\phi^{\gamma'}\mathbb{T}\mathbb{D}(h_i)^{\gamma'}\otimes\mathbb{D}(h'_j)^{\gamma}\mathbb{T}^{-1}.\end{aligned}$$

In the last step we used the fact that the commutation of the factors in a Kronecker product matrix implies a simple reordering of the basis, effected by the permutation matrix $\mathbb{T}$. Hence, the basis $s\psi^{\gamma}\otimes\phi^{\gamma'}$ carries the irrep of $H\otimes H'$ (equivalent to) $\gamma'\otimes\gamma$.

[1] D. Papoušek, J. M. R. Stone, and V. Špirko, J. Mol. Spectr. **48**, 17 (1973); D. Papoušek and M. R. Aliev, *Molecular Vibrational-Rotational Spectra* (Elsevier, Amsterdam, 1982).
[2] E. Zwart, H. Linnartz, W. L. Meerts, G. T. Fraser, D. D. Nelson, and W. Klemperer, J. Chem. Phys. **96**, 793 (1991).
[3] J. W. I. van Bladel, A. van der Avoird, and P. E. S. Wormer, J. Phys. Chem. **95**, 5414 (1991).
[4] D. D. Nelson, G. T. Fraser, and W. Klemperer, J. Chem. Phys. **83**, 6201 (1985).
[5] J. G. Loeser, C. A. Schmuttenmaer, R. C. Cohen, M. J. Elrod, D. W. Steyert, R. J. Saykally, R. E. Bumgarner, and G. A. Blake, J. Chem. Phys. **97**, 4727 (1992).
[6] M. Havenith, H. Linnartz, E. Zwart, A. Kips, J. J. ter Meulen, and W. L. Meerts, Chem. Phys. Lett. **193**, 261 (1992).
[7] E. H. T. Olthof, A. van der Avoird, and P. E. S. Wormer, J. Chem. Phys. **101**, 8430 (1994).
[8] J. W. I. van Bladel, A. van der Avoird, and P. E. S. Wormer, Chem. Phys. **165**, 47 (1992).
[9] P. R. Bunker, *Molecular Symmetry and Spectroscopy* (Academic, New York, 1979).
[10] D. J. Klein, C. H. Carlisle, and F. A. Matsen, Adv. Quantum Chem. **5**, 219 (1970).
[11] J. W. I. van Bladel, A. van der Avoird, P. E. S. Wormer, and R. J. Saykally, J. Chem. Phys. **97**, 4750 (1992).
[12] A. van der Avoird, P. E. S. Wormer, and R. Moszynski, Chem. Rev. (in press).
[13] C. H. Townes and A. L. Schawlow, *Microwave Spectroscopy* (McGraw-Hill, New York, 1955), Chap. 12.
[14] B. Jeziorski, W. Kołos, in *Molecular Interactions*, edited by H. Ratajczak and W. J. Orville-Thomas (Wiley, New York, 1982), Vol. 3, p. 1; B. Jeziorski, R. Moszynski, and K. Szalewicz (unpublished).
[15] L. Jansen and M. Boon, *Theory of Finite Groups. Applications in Physics* (North-Holland, Amsterdam, 1967), Chap. II.6.10.
[16] J. A. Odutola, T. R. Dyke, B. J. Howard, and J. S. Muenter, J. Chem. Phys. **70**, 4884 (1979).
[17] K. P. Sagarik, R. Ahlrichs, and S. Brode, Mol. Phys. **57**, 1247 (1986).
[18] E. H. T. Olthof, A. van der Avoird, and P. E. S. Wormer, J. Mol. Struct. (Theochem) **307**, 201 (1994).
[19] A. van der Avoird, E. H. T. Olthof, and P. E. S. Wormer, Faraday Discuss. Chem. Soc. **97** (1994).
[20] D. D. Nelson, W. Klemperer, G. T. Fraser, F. J. Lovas, and R. D. Suenram, J. Chem. Phys. **87**, 6364 (1987).
[21] H. Linnartz, A. Kips, W. L. Meerts, and M. Havenith, J. Chem. Phys. **99**, 2449 (1993).
[22] K. Balasubramanian, J. Chem. Phys. **72**, 665 (1980).
[23] J. A. Odutola, D. L. Alvis, C. W. Curtiss, and T. R. Dyke, Mol. Phys. **42**, 267 (1981).